Radiation from Multiple Circumferential Slots on a Conducting Circular Cylinder

Jong Kweon Park and Hyo Joon Eom, *Member, IEEE*

***Abstract*—Electromagnetic wave radiation from multiple circumferential slots on a conducting circular cylinder is theoretically investigated. The Fourier transform/series technique is used to represent the continuous and discrete modes of the scattered field. The mode matching is utilized to constitute a set of simultaneous equations for the discrete modal coefficients. The residue calculus is applied to transform the scattered-field integral representations into fast-converging series forms, thereby facilitating the numerical computations. Numerical computations illustrate the behavior of radiation in terms of the slot geometry, the incident mode, and the operating frequency.**

***Index Terms*—Electromagnetic radiation, slot antennas.**

I. Introduction

ELECTROMAGNETIC scattering from circumferential slots on a circular conducting cylinder is an important subject matter due to its antenna application [1], [2]. Radiation from a single circumferential slot on a coaxial cable was studied by Chang [3] to obtain an equivalent-circuit representation. The aperture admittance of a circumferential slot in a circular cylinder was obtained in [4] using Parseval's theorem. Knop and Libelo [5] investigated the leakage radiation from a circumferential slot on a conducting cylinder and its applications to the electromagnetic interference (EMI) problems. Recently, Xu and Wu [6] have considered radiation from an infinite number of circumferential slots on a conducting cylinder in order to apply to a millimeter-wave grating antenna. In this paper, we analyze scattering and radiation from a finite number of circumferential slots on a conducting cylinder using the Fourier transform and mode matching as used in [7]. Our analysis allows us to study the effects of the number of slots on the radiation and scattering behaviors. In Sections II and III, we present TE (transverse electric to propagation direction) and TM (transverse magnetic to propagation direction) wave scattering analyses and their applications to leaky-wave antenna. A brief summary on the scattering analysis is given in Section V.

II. TE-Wave Analysis

Consider multiple circumferential slots on a thick circular conducting cylinder as shown in Fig. 1. Assume the primary field (incident TE_{01} mode) propagates from below. Then the scattered electric field has a ϕ component only due to a circular symmetry. In region (I) ($\rho < a$), the total electric field is a sum of the incident and scattered field as

$$E^i_{\phi \mathrm{I}}(\rho, z) = \frac{i\omega\mu}{k_c} J_1(k_c\rho) e^{i\beta_z z} \tag{1}$$

$$E_{\phi \mathrm{I}}(\rho, z) = \frac{i\omega\mu}{2\pi} \int_{-\infty}^{\infty} \frac{1}{\kappa} \tilde{E}_{\mathrm{I}}(\zeta) J_1(\kappa\rho) e^{-i\zeta z}\, d\zeta \tag{2}$$

where $k_c = 3.832/a$, $\beta_z = \sqrt{\beta^2 - k_c^2}$, $\beta = \omega\sqrt{\mu\epsilon_r\epsilon_0} = 2\pi/\lambda$, $\kappa = \sqrt{\beta^2 - \zeta^2}$, $J_1(.)$ is the first order Bessel function. In region (II) ($a < \rho < b$), the electric field is a sum of the discrete modes as follows:

$$E_{\phi \mathrm{II}}(\rho, z) = \sum_{n=0}^{N-1} \sum_{k=1}^{\infty} \frac{-i\omega\mu}{\kappa_k} Q'(\kappa_k\rho) \sin a_k(z - nT) \times [u(z - nT) - u(z - d - nT)] \tag{3}$$

where $Q(\kappa_k\rho) = r_k^n J_0(\kappa_k\rho) + s_k^n N_0(\kappa_k\rho)$ and a prime denotes the differentiation with respect to $\kappa_k\rho$. The coefficients r_k^n and s_k^n are unknown to be determined by the boundary conditions $\kappa_k = \sqrt{\beta^2 - a_k^2}$, $a_k = k\pi/d$, and $u(.)$ is the unit step function. In region (III) ($\rho > b$), the electric field is

$$E_{\phi \mathrm{III}}(\rho, z) = \frac{i\omega\mu}{2\pi} \int_{-\infty}^{\infty} \frac{1}{\xi} \tilde{E}_{\mathrm{III}}(\zeta) H_1^{(1)}(\xi\rho) e^{-i\zeta z}\, d\zeta \tag{4}$$

where $\xi = \sqrt{\beta_0^2 - \zeta^2}$, $\beta_0 = \omega\sqrt{\mu\epsilon_0}$, and $H_1^{(1)}(.)$ is the first-order Hankel function of the first kind. Note that it is trivial to evaluate the corresponding H_z and H_ρ field components in each region. The E_ϕ field continuity at $\rho = a$ gives

$$E_{\phi \mathrm{I}}(a, z) = \begin{cases} E_{\phi \mathrm{II}}(a, z) & nT < z < d + nT \\ 0, & \text{otherwise.} \end{cases} \tag{5}$$

Taking the Fourier transform to (5), $\int_{-\infty}^{\infty} (5) e^{i\zeta z}\, dz$, yields

$$\tilde{E}_{\mathrm{I}}(\zeta) = -\sum_{n=0}^{N-1} \sum_{k=1}^{\infty} \frac{Q'(\kappa_k a)}{\kappa_k} \frac{\kappa F_k^n(\zeta)}{J_1(\kappa a)} \tag{6}$$

where

$$F_k^n(\zeta) = \frac{a_k[(-1)^k e^{i\zeta d} - 1]}{\zeta^2 - a_k^2} e^{i\zeta nT}. \tag{7}$$

The H_z field continuity at $\rho = a$ for $nT < z < d + nT$, $H^i_{z\mathrm{I}}(a, z) + H_{z\mathrm{I}}(a, z) = H_{z\mathrm{II}}(a, z)$, is written explicitly as

$$J_0(k_c a) e^{i\beta_z z} + \frac{1}{2\pi} \int_{-\infty}^{\infty} \tilde{E}_{\mathrm{I}}(\zeta) J_0(\kappa a) e^{-i\zeta z}\, d\zeta = \sum_{n=0}^{N-1} \sum_{k=1}^{\infty} Q(\kappa_k a) \sin a_k(z - nT). \tag{8}$$

Manuscript received October 13, 1997; revised June 25, 1998. This work was supported by the Satellite Technology Research Center of KAIST, Korea under Grant GD0083F.

The authors are with the Department of Electrical Engineering, Korea Advanced Institute of Science and Technology, Taejon, 305-701 Korea.

Publisher Item Identifier S 0018-926X(99)03730-8.

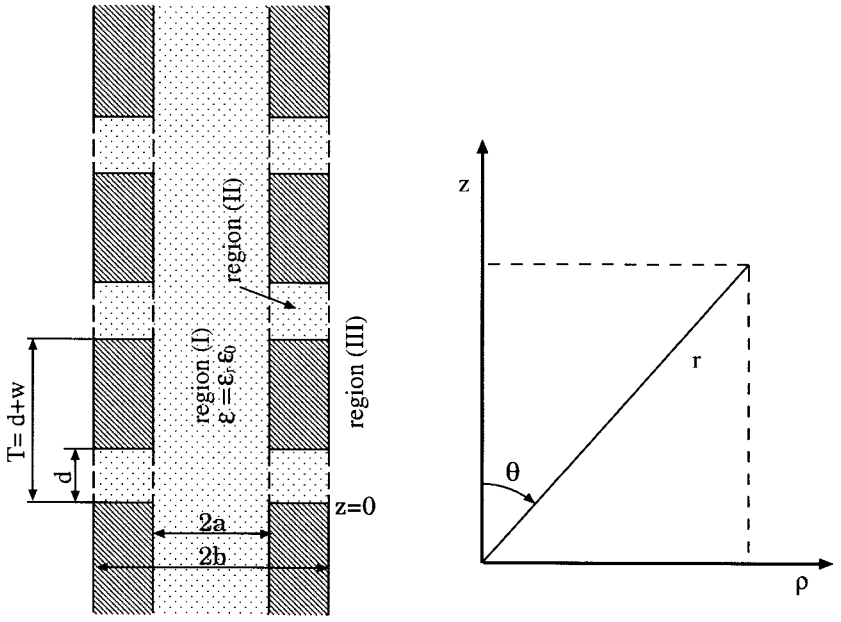

(a) (b)

Fig. 1. Multiple circumferential slot antenna on a circular cylinder. (a) Problem geometry. (b) Coordinate system.

Multiplying (8) by $\sin a_l(z-pT)$ and integrating with respect to z from pT to $d+pT$ and rearranging

$$\sum_{n=0}^{N-1}\sum_{k=1}^{\infty}\left[\frac{J_1(\kappa_k a)}{\kappa_k} I_{kl}^{np} - 0.5\,dJ_0(\kappa_k a)\delta_{kl}\delta_{np}\right] r_k^n + \sum_{n=0}^{N-1}\sum_{k=1}^{\infty}\left[\frac{N_1(\kappa_k a)}{\kappa_k} I_{kl}^{np} - 0.5\,dN_0(\kappa_k a)\delta_{kl}\delta_{np}\right] s_k^n = -J_0(k_c a)F_l^p(\beta_z). \tag{9}$$

Note that δ_{kl} is the Kronecker delta and

$$I_{kl}^{np} = \frac{1}{2\pi}\int_{-\infty}^{\infty} \frac{\kappa J_0(\kappa a)}{J_1(\kappa a)} F_k^n(\zeta)F_l^p(-\zeta)\,d\zeta. \tag{10}$$

Using the residue calculus, we transform (10) into rapidly converging series as shown in (11) at the bottom of the page. ζ_j are the roots of $J_1(\kappa a)|_{\zeta=\zeta_j} = 0$. Similarly, the tangential field continuities at $\rho = b$ yield

$$\sum_{n=0}^{N-1}\sum_{k=1}^{\infty}\left[\frac{J_1(\kappa_k b)}{\kappa_k} K_{kl}^{np} - 0.5\,dJ_0(\kappa_k b)\delta_{kl}\delta_{np}\right] r_k^n + \sum_{n=0}^{N-1}\sum_{k=1}^{\infty}\left[\frac{N_1(\kappa_k b)}{\kappa_k} K_{kl}^{np} - 0.5\,dN_0(\kappa_k b)\delta_{kl}\delta_{np}\right] s_k^n = 0 \tag{12}$$

where

$$K_{kl}^{np} = \frac{1}{2\pi}\int_{-\infty}^{\infty} \frac{\xi H_0^{(1)}(\xi b)}{H_1^{(1)}(\xi b)} F_k^n(\zeta)F_l^p(-\zeta)\,d\zeta. \tag{13}$$

An evaluation of K_{kl}^{np} with the contour integral technique [7] gives

$$K_{kl}^{np} = \frac{d}{2}\frac{\xi H_0^{(1)}(\xi b)}{H_1^{(1)}(\xi b)}\delta_{kl}\delta_{np}|_{\zeta=a_k} - a_k a_l\Big[\{1+(-1)^{k+l}\}I_{kl}^{(1)}(gT) - (-1)^k I_{kl}^{(1)}(d+gT) - (-1)^l I_{kl}^{(1)}(-d+gT)\Big] \tag{14}$$

where

$$I_{kl}^{(1)}(x) = -\frac{2}{\pi^2}\int_0^{\infty} \times \frac{e^{i\beta_0|x|}e^{-\beta_0 v|x|}}{\beta_0^3 b[(1+iv)^2-(a_k/\beta_0)^2][(1+iv)^2-(a_l/\beta_0)^2]} \times \frac{1}{J_1^2\left[\beta_0 b\sqrt{v(-2i+v)}\right] + N_1^2\left[\beta_0 b\sqrt{v(-2i+v)}\right]}\,dv \tag{15}$$

$$g = n - p. \tag{16}$$

From (9) and (12), we obtain the matrix equation for r_k^n and s_k^n

$$\begin{bmatrix}\Psi_1 & \Psi_2\\ \Psi_3 & \Psi_4\end{bmatrix}\begin{bmatrix}R\\ S\end{bmatrix} = \begin{bmatrix}\Gamma\\ 0\end{bmatrix} \tag{17}$$

$$I_{kl}^{np} = \frac{d}{2}\frac{\kappa J_0(\kappa a)}{J_1(\kappa a)}\delta_{kl}\delta_{np}|_{\zeta=a_k} - a_k a_l \sum_{j=1}^{\infty} \frac{i\kappa^2[\{(-1)^{k+l}+1\}e^{i\zeta|n-p|T} - (-1)^k e^{i\zeta|d+(n-p)T|} - (-1)^l e^{i\zeta|(n-p)T-d|}]}{a\zeta(\zeta^2-a_k^2)(\zeta^2-a_l^2)}\Bigg|_{\zeta=\zeta_j} \tag{11}$$

where R and S are column vectors of r_k^n and s_k^n, respectively, and Ψ_1, Ψ_2, Ψ_3, Ψ_4, and Γ elements are

$$\psi_{1,kl}^{np} = \frac{J_1(\kappa_k a)}{\kappa_k} I_{kl}^{np} - 0.5\, d J_0(\kappa_k a)\delta_{kl}\delta_{np} \tag{18}$$

$$\psi_{2,kl}^{np} = \frac{N_1(\kappa_k a)}{\kappa_k} I_{kl}^{np} - 0.5\, d N_0(\kappa_k a)\delta_{kl}\delta_{np} \tag{19}$$

$$\psi_{3,kl}^{np} = \frac{J_1(\kappa_k b)}{\kappa_k} K_{kl}^{np} - 0.5\, d J_0(\kappa_k b)\delta_{kl}\delta_{np} \tag{20}$$

$$\psi_{4,kl}^{np} = \frac{N_1(\kappa_k b)}{\kappa_k} K_{kl}^{np} - 0.5\, d N_0(\kappa_k b)\delta_{kl}\delta_{np} \tag{21}$$

$$\gamma_l^p = \frac{-a_l[(-1)^l e^{i\beta_z d} - 1]}{\beta_z^2 - a_l^2} J_0(k_c a) e^{i\beta_z pT}. \tag{22}$$

In low-frequency limit, an approximate closed-form solution for a single slot $N = 1$ is

$$r_1^0 \approx \frac{\psi_{4,11}^{00}\gamma_1^0}{(\psi_{1,11}^{00}\psi_{4,11}^{00} - \psi_{2,11}^{00}\psi_{3,11}^{00})} \tag{23}$$

$$s_1^0 \approx \frac{-\psi_{3,11}^{00}\gamma_1^0}{(\psi_{1,11}^{00}\psi_{4,11}^{00} - \psi_{2,11}^{00}\psi_{3,11}^{00})} \tag{24}$$

and the remaining $r_k^0 \approx s_k^0 \approx 0$. By use of the residue calculus, we evaluate the scattered field at $z = \pm\infty$ in region (I)

$$E_{\phi \mathrm{I}}(\rho, \pm\infty) = \sum_{j=1}^{\infty} L_j^{\pm}(\zeta) \frac{i\omega\mu}{\kappa} J_1(\kappa\rho) e^{\pm i\zeta z}|_{\zeta=\zeta_j} \tag{25}$$

where

$$L_j^{\pm}(\zeta) = \sum_{n=0}^{N-1}\sum_{k=1}^{\infty} \frac{i a_k Q'(\kappa_k a)}{\kappa_k a} \frac{\kappa^2[(-1)^k e^{\mp i\zeta d} - 1]}{\zeta J_0(\kappa a)(\zeta^2 - a_k^2)} e^{\mp i\zeta nT} \tag{26}$$

ζ_j is determined by $J_1(\kappa a)|_{\zeta=\zeta_j} = 0$. Let P_i, P_r, P_t, and P_s denote the time-averaged incident, reflected, transmitted, and radiated powers, respectively. Then the reflection (η), transmission (τ), and scattering (σ) coefficients are

$$\begin{aligned}\tau &= \frac{P_t}{P_i} \\ &= \left|1 + L_j^+(\zeta_j)\right|^2_{\zeta_j=\beta_z} \\ &\quad + \sum_{\zeta_j \neq \beta_z} \frac{k_c^2 \operatorname{Re}[\zeta_j] J_1^2(\kappa a) - J_0(\kappa a) J_2(\kappa a)}{\kappa^2 \operatorname{Re}[\beta_z] J_0^2(k_c a)} \left|L_j^+(\zeta_j)\right|^2\end{aligned} \tag{27}$$

$$\sigma = \frac{P_s}{P_i} \tag{28}$$

$$\begin{aligned}\eta &= \frac{P_r}{P_i} \\ &= \sum_{j=1}^{\infty} \frac{k_c^2 \operatorname{Re}[\zeta_j] J_1^2(\kappa a) - J_0(\kappa a) J_2(\kappa a)}{\kappa^2 \operatorname{Re}[\beta_z] J_0^2(k_c a)} \left|L_j^-(\zeta_j)\right|^2\end{aligned} \tag{29}$$

where

$$P_i = \frac{\pi a^2 \omega\mu}{2k_c^2} J_0^2(k_c a) \operatorname{Re}[\beta_z] \tag{30}$$

$$P_s = \frac{\pi b d}{2} \operatorname{Re}\left[\sum_{n=0}^{N-1}\sum_{k=1}^{\infty} \frac{-i\omega\mu}{\kappa_k} Q'(\kappa_k b) Q^*(\kappa_k b)\right]. \tag{31}$$

The symbol $\operatorname{Re}[.]$ denotes taking the real part of $[.]$, $*$ denotes complex conjugate, and the power conservation requires $\eta + \tau + \sigma = 1$. The far-zone radiation field at distance r is

$$E_{\phi \mathrm{III}}(r, \theta) = K_s^{\mathrm{TE}}(\theta) \frac{e^{i(\beta_0 r - \pi)}}{r} \tag{32}$$

where

$$\begin{aligned}K_s^{\mathrm{TE}}(\theta) = \sum_{n=0}^{N-1}\sum_{k=1}^{\infty} &\frac{Q'(\kappa_k b)}{\pi\kappa_k} \\ &\times \frac{i\omega\mu a_k[1 - (-1)^k e^{-i\beta_0 d\cos\theta}]}{H_1^{(1)}(\beta_0 b \sin\theta)[(\beta_0\cos\theta)^2 - a_k^2]} \\ &\times e^{-i\beta_0 nT\cos\theta}.\end{aligned} \tag{33}$$

III. TM-Wave Analysis

Assume the primary field (incident TM_{01} mode) propagates from below the slotted circular cylinder shown in Fig. 1. In region (I) ($\rho < a$), the magnetic field consists of

$$H_{\phi \mathrm{I}}^i(\rho, z) = \frac{-i\omega\epsilon}{k_c} J_1(k_c\rho) e^{i\beta_z z} \tag{34}$$

$$H_{\phi \mathrm{I}}(\rho, z) = \frac{-i\omega\epsilon}{2\pi} \int_{-\infty}^{\infty} \frac{1}{\kappa} \tilde{E}_{\mathrm{I}}(\zeta) J_1(\kappa\rho) e^{-i\zeta z}\, d\zeta \tag{35}$$

where $k_c = 2.405/a$, $\beta_z = \sqrt{\beta^2 - k_c^2}$, $\beta = \omega\sqrt{\mu\epsilon_r\epsilon_0}$, $\kappa = \sqrt{\beta^2 - \zeta^2}$. In region (II) ($a < \rho < b$), the magnetic field can be expressed as follows:

$$\begin{aligned}H_{\phi \mathrm{II}}(\rho, z) = \sum_{n=0}^{N-1}\sum_{m=0}^{\infty} &\frac{i\omega\epsilon}{\kappa_m} R_0'(\kappa_m\rho)\cos a_m(z - nT) \\ &\times [u(z - nT) - u(z - d - nT)]\end{aligned} \tag{36}$$

where $R_0(\kappa_m\rho) = p_m^n J_0(\kappa_m\rho) + q_m^n N_0(\kappa_m\rho)$, $\kappa_m = \sqrt{\beta^2 - a_m^2}$, and $a_m = m\pi/d$. In region (III) ($\rho > b$)

$$H_{\phi \mathrm{III}}(\rho, z) = \frac{-i\omega\epsilon_0}{2\pi} \int_{-\infty}^{\infty} \frac{1}{\xi} \tilde{E}_{\mathrm{III}}(\zeta) H_1^{(1)}(\xi\rho) e^{-i\zeta z}\, d\zeta \tag{37}$$

where $\xi = \sqrt{\beta_0^2 - \zeta^2}$, $\beta_0 = \omega\sqrt{\mu\epsilon_0}$. The applications of the boundary conditions are somewhat similar to those in the TE case. The E_z and H_ϕ field continuities at $\rho = a$ between regions (I) and (II) give

$$\begin{aligned}&\sum_{n=0}^{N-1}\sum_{m=0}^{\infty}\left[J_0(\kappa_m a) J_{ms}^{np} - 0.5\, d \frac{J_1(\kappa_m a)}{\kappa_m} \alpha_m \delta_{ms}\delta_{np}\right] p_m^n \\ &\quad + \sum_{n=0}^{N-1}\sum_{m=0}^{\infty}\left[N_0(\kappa_m a) J_{ms}^{np} - 0.5\, d \frac{N_1(\kappa_m a)}{\kappa_m} \right. \\ &\qquad \left. \times\, \alpha_m \delta_{ms}\delta_{np}\right] q_m^n \\ &\quad = -\frac{J_1(k_c a)}{k_c} G_s^p(\beta_z)\end{aligned} \tag{38}$$

where $\alpha_m = 2$, $(m = 0)$, $1(m = 1, 2, 3, \cdots)$ and

$$J_{ms}^{np} = \frac{1}{2\pi} \int_{-\infty}^{\infty} \frac{J_1(\kappa a)}{\kappa J_0(\kappa a)} G_m^n(\zeta) G_s^p(-\zeta)\, d\zeta \tag{39}$$

$$G_m^n(\zeta) = \frac{-i\zeta[(-1)^m e^{i\zeta d} - 1]}{\zeta^2 - a_m^2} e^{i\zeta nT}. \tag{40}$$

It is possible to transform (39) into a rapidly-converging series form by using the residue calculus. Similarly E_z and H_ϕ field continuities at $\rho = b$ between regions (II) and (III) yield

$$\sum_{n=0}^{N-1}\sum_{m=0}^{\infty}\left[J_0(\kappa_m b)L_{ms}^{np} - 0.5\epsilon_r\, d\,\frac{J_1(\kappa_m b)}{\kappa_m}\,\alpha_m\delta_{ms}\delta_{np}\right]p_m^n + \sum_{n=0}^{N-1}\sum_{m=0}^{\infty}\left[N_0(\kappa_m b)L_{ms}^{np} - 0.5\epsilon_r\, d\,\frac{N_1(\kappa_m b)}{\kappa_m} \times \alpha_m\delta_{ms}\delta_{np}\right]q_m^n = 0 \tag{41}$$

where

$$L_{ms}^{np} = \frac{1}{2\pi}\int_{-\infty}^{\infty}\frac{H_1^{(1)}(\xi b)}{\xi H_0^{(1)}(\xi b)}\,G_m^n(\zeta)G_s^p(-\zeta)\,d\zeta. \tag{42}$$

It is expedient to change (42) into a numerically efficient form by using the residue calculus. The scattered field at $z = \pm\infty$ in region (I) is

$$H_{\phi\mathrm{I}}(\rho, \pm\infty) = \sum_{j=1}^{\infty} L_j^{\pm}(\zeta)\,\frac{-i\omega\epsilon}{\kappa}\,J_1(\kappa\rho)e^{\pm i\zeta z}|_{\zeta=\zeta_j} \tag{43}$$

where

$$L_j^{\pm}(\zeta) = \mp\sum_{n=0}^{N-1}\sum_{m=0}^{\infty}\frac{R_0(\kappa_m a)}{a} \times \frac{\kappa[(-1)^m e^{\mp i\zeta d} - 1]}{J_1(\kappa a)(\zeta^2 - a_m^2)}\,e^{\mp i\zeta nT} \tag{44}$$

ζ_j is determined by $J_0(\kappa a)|_{\zeta=\zeta_j} = 0$. Similarly, the reflection (η), transmission (τ), and scattering (σ) coefficients are

$$\tau = \frac{P_t}{P_i} = \left|1 + L_j^{+}(\zeta_j)\right|^2_{\zeta_j=\beta_z} + \sum_{\zeta_j\neq\beta_z}\frac{k_c^2\,\mathrm{Re}[\zeta_j]J_1^2(\kappa a) - J_0(\kappa a)J_2(\kappa a)}{\kappa^2\,\mathrm{Re}[\beta_z]J_1^2(k_c a)}\left|L_j^{+}(\zeta_j)\right|^2 \tag{45}$$

$$\sigma = \frac{P_s}{P_i} \tag{46}$$

$$\eta = \frac{P_r}{P_i} = \sum_{j=1}^{\infty}\frac{k_c^2\,\mathrm{Re}[\zeta_j]J_1^2(\kappa a) - J_0(\kappa a)J_2(\kappa a)}{\kappa^2\,\mathrm{Re}[\beta_z]J_1^2(k_c a)}\left|L_j^{-}(\zeta_j)\right|^2 \tag{47}$$

where

$$P_i = \frac{\pi a^2\omega\epsilon}{2k_c^2}\,J_1^2(k_c a)\,\mathrm{Re}[\beta_z] \tag{48}$$

$$P_s = \frac{\pi b d}{2}\,\mathrm{Re}\left[\sum_{n=0}^{N-1}\sum_{m=0}^{\infty}\frac{i\omega\epsilon\alpha_m}{\kappa_m^*}\,R_0(\kappa_m b)R_0'(\kappa_m b)^*\right]. \tag{49}$$

The far-zone radiation field at distance r is

$$H_{\phi\mathrm{III}}(r, \theta) = K_s^{\mathrm{TM}}(\theta)\,\frac{e^{i(\beta_0 r - \pi)}}{r} \tag{50}$$

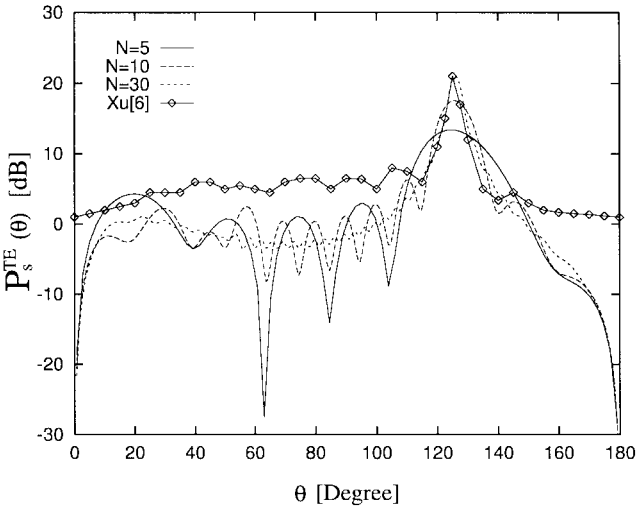

Fig. 2. Angular radiation pattern as a function of slot number N (TE wave) ($f = 36.5$ GHz, $\epsilon_r = 2.1$, $a = 5$ mm, $b/a = 1$, $T = 4.8$ mm, $d/T = 0.75$).

where

$$K_s^{\mathrm{TM}}(\theta) = \sum_{n=0}^{N-1}\sum_{m=0}^{\infty}\frac{R_0(\kappa_m b)}{\pi\tan\theta} \times \frac{\omega\epsilon_0[(-1)^m e^{-i\beta_0 d\cos\theta} - 1]}{H_0^{(1)}(\beta_0 b\sin\theta)[(\beta_0\cos\theta)^2 - a_m^2]} \times e^{-i\beta_0 nT\cos\theta}. \tag{51}$$

IV. Numerical Computations

The behavior of the TE-wave radiation from an infinite number of slots $(N = \infty)$ was well understood in [6]. In Fig. 2, we show the TE-wave angular radiation pattern $P_s^{\mathrm{TE}}(\theta) = 20\log|K_s^{\mathrm{TE}}(\theta)/[K_s^{\mathrm{TE}}(90°)|_{N=20}]|$ for different slot number N. As N increases, the main-lobe beamwidth and the sidelobe level decrease. When $N = 30$, the angular radiation pattern agrees well with the results in [6] for $110° < \theta < 140°$. In our computation, we use one propagation mode $(k, l = 1)$ in (18), thus confirming the energy conservation to within 0.01% error. Our computational experience indicates that all propagating modes in region (II), $(\beta > a_k)$, must be used in computation with (18) in order to achieve numerical accuracy and convergence. Fig. 3 illustrates the TE-wave angular radiation pattern

$$P_s^{TE}(\theta) = 20\log\left|\left[\frac{fK_s^{\mathrm{TE}}(\theta)}{\sqrt{P_i}}\right]\Big/\left[\frac{f_0 K_s^{\mathrm{TE}}(90°)}{\sqrt{P_i}}\right]_{f_0=36\ \mathrm{GHz}}\right|$$

for different operating frequency f. The main lobe locations of each curve agree well with the results in [6], but the angular radiation pattern, in general, changes substantially as the operating frequency changes from 32 to 40 GHz. Fig. 4 shows the behavior of the reflection, transmission, and scattering coefficients versus the number of slots. Note that the radiation efficiency (scattering coefficient) exceeds 92% when $N > 18$. Fig. 5 shows the angular radiation pattern

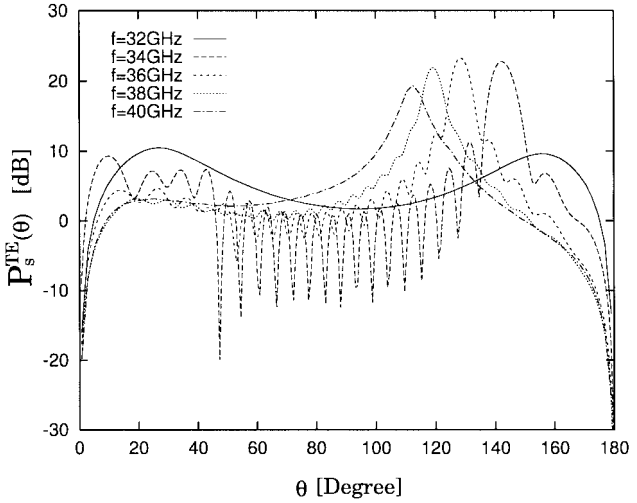

Fig. 3. Frequency scanning characteristics (TE wave) ($\epsilon_r = 2.1$, $a = 5$ mm, $b/a = 1$, $T = 4.8$ mm, $d/T = 0.75$, $N = 20$).

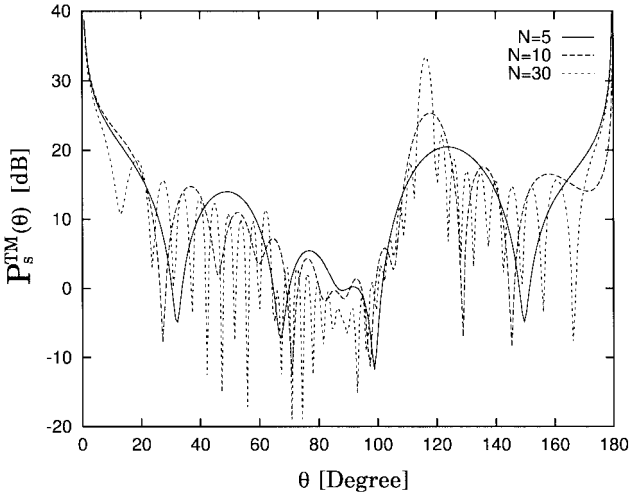

Fig. 5. Angular radiation pattern as a function of slot number N (TM wave) ($f = 36.5$ GHz, $\epsilon_r = 2.1$, $a = 5$ mm, $b/a = 1$, $T = 4.8$ mm, $d/T = 0.4$).

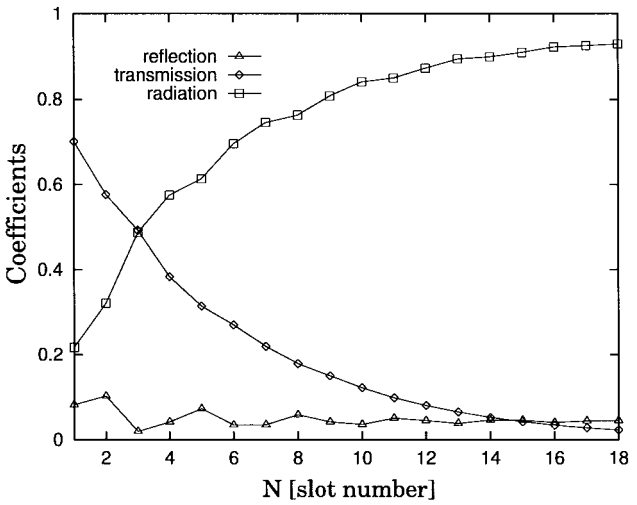

Fig. 4. Reflection, transmission, and scattering coefficients versus slot number N (TE wave) ($f = 36.5$ GHz, $\epsilon_r = 2.1$, $a = 5$ mm, $b/a = 1$, $T = 4.8$ mm, $d/T = 0.75$).

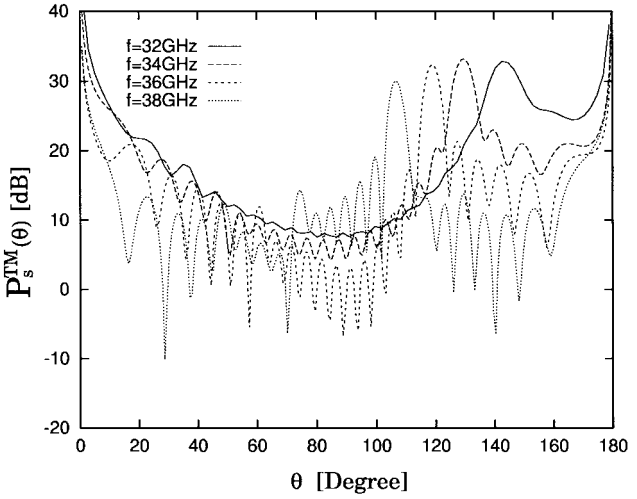

Fig. 6. Frequency scanning characteristics (TM wave) ($\epsilon_r = 2.1$, $a = 5$ mm, $b/a = 1$, $T = 4.8$ mm, $d/T = 0.4$, $N = 20$).

$P_s^{\mathrm{TM}}(\theta) = 20 \log |K_s^{\mathrm{TM}}(\theta)/[K_s^{\mathrm{TM}}(90°)|_{N=20}]|$ for the TM wave. All parameters used in the computations are chosen to maximize the radiation as used in [6]. As the slot number N increases, the main-lobe beamwidth near $\theta = 118°$ becomes narrower while the antenna pattern still retains the endfire characteristics with the peaked radiation at $\theta = 0°$ and 180°. Fig. 6 illustrates the TM-wave radiation pattern

$$P_s^{\mathrm{TM}}(\theta) = 20 \log \left| \left[\frac{f K_s^{\mathrm{TM}}(\theta)}{\sqrt{P_i}} \right] \Big/ \left[\frac{f_0 K_s^{\mathrm{TM}}(90°)}{\sqrt{P_i}} \right]_{f_0 = 36\ \mathrm{GHz}} \right|$$

for different operating frequency f. As the frequency changes from 32 to 38 GHz, the location of the main lobe is seen to shift slightly less than 40°.

V. Conclusion

Using the Fourier transform and the mode-matching method, we analyze the radiation characteristics of the multiple circumferential slots on a conducting circular cylinder. The effects of the number of the slots on the angular radiation pattern are investigated for the TE and TM waves. The presented solution is formulated in terms of the fast-converging series, which are amenable to numerical computations. Our numerical computations for the radiation pattern agree reasonably with the antenna measurements at Ka band. Our formulation is useful for the design of the circumferential slot antenna, which has no azimuthal variation.

References

[1] C. H. Papas, "Radiation from a transverse slot in an infinite cylinder," *J. Math. Phys.*, vol. 28, pp. 227–236, Jan. 1950.
[2] J. R. Wait, *Electromagnetic Radiation from Cylindrical Structures.* Elmsford, NY: Pergamon, 1959.
[3] D. C. Chang, "Equivalent-circuit representation and characteristics of a radiating cylinder driven through a circumferential slot," *IEEE Trans. Antennas Propagat.*, vol. AP-21, pp. 792–796, Nov. 1973.
[4] S. Papatheodorou, J. R. Mautz, and R. F. Harrington, "The aperture admittance of a circumferential slot in a circular cylinder," *IEEE Trans. Antennas Propagat.*, vol. 40, pp. 240–244, Feb. 1992.
[5] C. M. Knop and L. F. Libelo, "On the leakage radiation from a circumferentially-slotted cylinder and its application to the EMI pro-

duced by TEM-coaxial rotary joints," *IEEE Trans. Electromagn. Compat.*, vol. 37, pp. 583–589, Nov. 1995.
[6] S. Xu and X. Wu, "Millimeter-wave omnidirectional dielectric rod metallic grating antenna," *IEEE Trans. Antennas Propagat.*, vol. 44, pp. 74–79, Jan. 1996.
[7] J. K. Park and H. J. Eom, "Fourier transform analysis of dielectric-filled edge-slot antenna," *Radio Sci.*, vol. 32, no. 6, pp. 2149–2154, Nov./Dec. 1997; correction to "Fourier transform analysis of dielectric-filled edge-slot antenna," vol. 33, no. 3, p. 631, May/June 1998.

Jong Kweon Park was born in Korea in 1969. He received the B.S. degree in electronic engineering from the Kyungpook National University, Taegu, Korea, in 1994, and the M.S. degree in electrical engineering from the Korea Advanced Institute of Science and Technology, Taejon, in 1997. He is now working toward the Ph.D. degree in electrical engineering at the Korea Advanced Institute of Science and Technology at Taejon, Korea.

His research interests include wave scattering and antenna analysis.

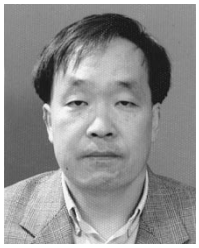

Hyo Joon Eom (S'78–M'82) received the B.S. degree in electronic engineering from Seoul National University, Korea, and the M.S. and Ph.D. degrees in electrical engineering from the University of Kansas, Lawrence, in 1977 and 1982, respectively.

From 1981 to 1984, he was a Research Associate at the Remote Sensing Laboratory of the University of Kansas. From 1984 to 1990 he was with the Faculty of the Department of Electrical Engineering and Computer Science, University of Illinois, Chicago. In 1989 he joined the Department of Electrical Engineering, Korea Advanced Institute of Science and Technology where he is currently a Professor. His research interests include wave scattering and antenna.